Quantitative interaction proteomics reveals differences in the interactomes of amyloid precursor protein isoforms

DOI:
10.1111/jnc.14666

Document Version
Accepted author manuscript

Quantitative interaction proteomics reveals differences in the interactomes of amyloid precursor protein isoforms

Robert J. Andrew[1*], Kate Fisher[1], Kate J. Heesom[2], Katherine A. B. Kellett[1] and Nigel M. Hooper[1]

[1] Division of Neuroscience and Experimental Psychology, School of Biological Sciences, Faculty of Biology, Medicine and Health, University of Manchester, Manchester Academic Health Science Centre, Oxford Road, Manchester, M13 9PL, UK

[2] Proteomics Facility, Faculty of Medical and Veterinary Sciences, University of Bristol, Bristol BS8 1TD, UK

[*]**Current address:** Department of Neurobiology, The University of Chicago, Chicago, IL 60637, USA

Address correspondence and reprint requests to Nigel Hooper, Division of Neuroscience and Experimental Psychology, School of Biological Sciences, Faculty of Biology, Medicine and Health, AV Hill Building, University of Manchester, Oxford Road, Manchester, M13 9PL, UK. E-mail: nigel.hooper@manchester.ac.uk

Running title: APP isoform interactomes

Keywords: Amyloid precursor protein, interactome, amyloid-β, proteolysis, SILAC, GAP43, .

Abbreviations: Aβ, amyloid-β; AD, Alzheimer's disease; AICD, amyloid precursor protein intracellular domain; APP, amyloid precursor protein; BACE1, β-site APP cleaving enzyme 1; BCA; bicinchoninic acid; CTF, C-terminal fragment; KPI, Kunitz protease inhibitor; LC-MS/MS, liquid chromatography-tandem mass spectrometry; MAMs, mitochondria associated endoplasmic reticulum membranes; sAPPα, soluble APP resulting from α-secretase cleavage; sAPPβ, soluble APP resulting from β-secretase cleavage; SILAC, stable isotope labelling of amino acids in cell culture, RRID, research resource identifier (see scicrunch.org).

Abstract

The generation of the amyloid-β (Aβ) peptides from the amyloid precursor protein (APP) through sequential proteolysis by β- and γ-secretases is a key pathological event in the initiation and propagation of Alzheimer's disease. Aβ and the transcriptionally active APP intracellular domain (AICD) are generated preferentially from the APP695 isoform compared to the longer APP751 isoform. As the Aβ and AICD produced from cleavage of APP695 and APP751 are identical we hypothesised that the two isoforms have differences within their interactomes which mediate the differential processing of the two isoforms. To investigate this, we applied a proteomics-based approach to identify differences in the interactomes of the APP695 and APP751 isoforms. Using stable isotope labelling of amino acids in cell culture (SILAC) and quantitative proteomics, we compared the interactomes of APP695 and APP751 expressed in human SH-SY5Y cells. Through this approach, we identified enrichment of proteins involved in mitochondrial function, the nuclear pore and nuclear transport specifically in the APP695 interactome. Further interrogation of the APP interactome and subsequent experimental validation (co-immunoprecipitation and siRNA knockdown) revealed GAP43 as a specific modulator of APP751 proteolysis, altering Aβ generation. Our data indicate that interrogation of the APP interactome can be exploited to identify proteins which influence APP proteolysis and Aβ production in an isoform dependent-manner.

Introduction

Alzheimer's disease (AD) is characterised by the deposition in the brain of plaques containing the peptide amyloid-β (Aβ) (Masters *et al.* 1985). Aβ is postulated to be the neurotoxic moiety which triggers the complex series of events leading to the neurodegeneration in AD (De Strooper & Karran 2016). Aβ is derived from the amyloid precursor protein (APP) following its sequential proteolysis by the β- and γ-secretases (Andrew *et al.* 2016). In this amyloidogenic pathway, proteolytic cleavage by the β-secretase (β-site APP cleaving enzyme 1; BACE1) releases soluble APPβ (sAPPβ) and subsequent cleavage of the membrane bound C-terminal fragment (CTF) by γ-secretase liberates Aβ and the APP intracellular domain (AICD). Alternatively, non-amyloidogenic proteolysis by α-secretases such as ADAM10 releases sAPPα, and subsequent proteolysis of the remaining CTF by γ-secretase liberates the soluble fragment p3 and AICD (Andrew *et al.* 2016).

Alternative splicing of APP mRNA produces isoforms of various lengths. Due to their expression within the brain, the main isoforms of interest to AD are APP695, APP751 and APP770, comprising 695, 751 and 770 amino acids, respectively. Exon 7 of the *APP* gene codes for a 56 amino acid Kunitz-type protease inhibitor (KPI) domain with 50% sequence homology with the Kunitz family of serine protease inhibitors that is present in both APP751 and APP770 (Sandbrink *et al.* 1996). An additional 19 amino acid domain with sequence homology to the OX-2 antigen of thymus derived lymphoid cells is coded for by exon 8 of the *APP* gene and is only present in the APP770 isoform (Sandbrink *et al.* 1996). Reports have previously identified alterations in the expression levels of different APP isoforms in AD (Golde *et al.* 1990; Matsui *et al.* 2007; Moir *et al.* 1998), though the cause and consequence of these alterations have yet to be established. The different APP isoforms have been shown to undergo differential proteolysis, with Aβ being produced preferentially, and transcriptionally active AICD produced specifically, from the APP695 isoform (Belyaev *et al.* 2010; Grimm *et al.* 2015; Pardossi-Piquard *et al.* 2005).

APP has been postulated to have a wide range of roles (Reinhard *et al.* 2005), including in cell-cell adhesion (Soba *et al.* 2005), synaptogenesis (Wang *et al.* 2009) and as a cell surface receptor (Rice *et al.* 2013). APP is dynamically trafficked within neurons, and its subcellular location has been reported to influence its spatial proximity to the secretases responsible for its proteolysis (Haass *et al.* 2012). A wide range of proteins have been reported to directly interact with APP, some of which influence its proteolysis and thus, the generation of Aβ (Perreau *et al.* 2010; Andrew *et al.* 2016). APP interactomic studies have been carried out in both AD post-mortem brain tissue (Cottrell *et al.* 2005) and transgenic mouse models of AD (Bai *et al.* 2008; Kohli *et al.* 2012) highlighting potential functions and trafficking mechanisms involving APP, as well as elucidating novel interactions which influence APP proteolysis. Interactome studies also have the capacity to elucidate both functional networks and subcellular locations through 'guilt by association' allowing inference of a specific function for the candidate protein (Perreau *et al.* 2010). Interactome analysis has previously been used

to identify interactors of the γ-secretase complex (Wakabayashi *et al.* 2009) and BACE1 (He *et al.* 2004) which influence their ability to proteolytically cleave APP.

Here we have undertaken an unbiased mass spectrometry-based approach, using stable isotope labelling of amino acids in cell culture (SILAC) followed by APP immunoprecipitation and liquid chromatography-tandem mass spectrometry (LC-MS/MS) to identify the interaction networks of the two APP isoforms, APP695 and APP751, in human SH-SY5Y neuroblastoma cells. Through this approach, for the first time in a neuronal cell model, we identified enrichment of proteins implicated in nuclear import and mitochondrial function specifically in the APP695 interactome. In addition, we identified that GAP43 selectively interacts with the APP751 isoform and that its knockdown in SH-SY5Y cells specifically reduced proteolysis of the APP751 isoform.

Materials and methods

The study was not pre-registered and institutional approval was not required to conduct this work.

Cell culture and SILAC

SH-SY5Y cells (RRID:CVCL_0019, a kind gift from Dr Peter Vaughn, University of Leeds. Authenticated by short tandem repeat (STR) genotyping on 1st July 2015 by the DNA Sequencing Facility, University of Manchester), found to be 100% identical to SH-SY5Y cell line ATCC:CRL-2266a and not listed a commonly misidentified cell line by the International Cell Line Authentication Committee) were transfected with the cDNA encoding a C-terminally FLAG-tagged version of either wild type human APP695 or APP751 within the vector pIREShyg (Accession #U89672, Clontech, #6061-1) or mock transfected with empty pIREShyg vector by electroporation. Colonies expressing the desired constructs were selected by treatment with 75 μg/ml hygromycin (Invitrogen, #10687010) for 10 days. Use of the pIREShyg vector circumvents the requirement for continued treatment of cells with a selection antibiotic following the initial selection period. Cells were maintained in Dulbecco's Modified Eagle's Medium (DMEM) (Lonza, #BE12-604F) supplemented with 10% foetal bovine serum (FBS) (Gibco, #F9665) at 37°C with 5% CO_2. For SILAC labelling, cells were cultured in DMEM containing isotope labelled versions of the amino acids arginine (R) and lysine (K) and 10% dialysed FBS (Dundee Cell Products, #D-FBS). Mock transfected cells, APP695-FLAG expressing cells and APP751-FLAG expressing cells were cultured in heavy-labelled (R10, K8) DMEM (Dundee Cell Products, #LM015), medium-labelled (R6, K4) DMEM (Dundee Cell Products, LM-016) or light (R0, K0) DMEM (Dundee Cell Products, #LM-019), respectively, for a 3-week period. Over this period 6-8 passages were required indicating over 5 cell divisions which should ensure >95% labelling of the proteins (Munday *et al.* 2012).

Immunofluorescence microscopy

Cells were seeded into 24-well plates containing coverslips at 30,000 cells per well and cultured for 48 h. Cells were briefly washed in PBS then fixed and permeabilised with a 1:1 ratio of ice cold methanol and acetone for 10 min at room temperature. The cells were then washed in PBS and blocked in PBS containing 5% (v/v) fish skin gelatin (FSG) (Sigma, #G7765) for 1 h at room temperature. Coverslips were incubated with anti-FLAG (RRID:AB_259529, 1:500 mouse IgG, Sigma, #F3165) and anti-TGN-46 (1: 750, rabbit IgG, a kind gift from Dr Sreenivasan Ponambalam, University of Leeds) primary antibody overnight at 4^{o}C PBS containing 5% (w/v) FSG. Coverslips were washed three times in PBS containing 0.2% (v/v) Tween-20 (PBST) and incubated with anti-mouse Alexa Fluor 488 secondary antibody (RRID:AB_141607, 1:500 donkey IgG, Invitrogen, #A-21202) in PBS containing 5% FSG for 1 h at room temperature. Coverslips were washed once in PBS and incubated with DAPI (Cell Signalling Technology, #4083S) at 1:1000 in PBS for 2 min at room temperature. The coverslips were then washed twice in PBST and once with PBS before being mounted using Fluoromount G (Cambridge Biosciences, #0100-01). Images were acquired on a DeltaVision [RT] (Applied Precision) restoration microscope and analysed using Image J software (National Institutes of Health).

Cell lysis

Cells were washed in ice cold phosphate buffered saline (PBS) (Lonza, #BE17-513F), harvested and pelleted by centrifugation at 500 x g for 5 min. Cells were subsequently lysed on ice for 30 min in lysis buffer (10 mM Tris-HCl pH7.5, 150 mM NaCl, 0.5% (v/v) Nonidet P-40, 1x EDTA-free protease inhibitor cocktail). The cell lysates were clarified by centrifugation at 12,460 x g for 10 min and the protein concentration was determined by bicinchoninic acid (BCA) assay.

Anti-FLAG affinity gel co-immunoprecipitation

Anti-FLAG affinity gel (Sigma, #A2220) was washed twice in PBS and subsequently equilibrated in lysis buffer for 30 min. Immunoprecipitation was then carried out on 1mg of total cell lysate from each cell line in a total volume of 1 ml. Lysates were diluted, added to the affinity resin and incubated at 4°C for 2 h on a rotary mixer. The gel was pelleted by centrifugation at 500 x g for 1 min and the supernatant was removed as the unbound fraction. The gel was subsequently washed three times in PBS and then re-suspended in 2x dissociation buffer (200 mM Tris-HCl, 4% (w/v) sodium dodecyl sulphate, 20% (v/v) glycerol, 200 mM dithiothreitol, 0.04% bromophenol blue pH 6.8) and boiled for 5 min to elute the immunoprecipitated proteins.

Co-immunoprecipitations

Cells were lysed and the protein concentration was determined as described above. Anti-FLAG affinity gel or Protein G Dynabeads (Life Technologies, #10004D) with anti-FLAG or anti-GAP43

(RRID:AB_1310252, Abcam, #ab75810) were used for immunoprecipitations. Dynabeads (1.5 µg) were incubated with 2.5 µg of antibody diluted in 200 µl of PBS containing 0.02% Tween-20 for 1 h. The supernatant was removed and the Dynabeads washed twice in 500 µl of PBS containing 0.02% Tween. Cell lysates were diluted to 1 mg/ml and 1 mg of total cell lysate was incubated with the anti-FLAG affinity gel or Dynabeads at 4°C for 2 h. The supernatants were removed and saved as unbound fractions and the anti-FLAG affinity gel and Dynabeads washed 3 times in 500 µl of PBS containing 0.02% Tween-20. The pellet was then re-suspended in 50 µl of 1x dissociation buffer (100 mM Tris-HCl, 2% (w/v) sodium dodecyl sulphate, 10% (v/v) glycerol, 100 mM dithiothreitol, (0.02%) (w/v) bromophenol blue, pH 6.8) and boiled for 5 min to elute the immunoprecipitated proteins.

Sample digestion and quantitative mass spectrometry

Proteins samples were separated by SDS-PAGE. The gel lane was cut into 3 slices and each slice subjected to in-gel tryptic digestion using a DigestPro automated digestion unit (Intavis Ltd.). The resulting peptides were fractionated using an Ultimate 3000 nanoHPLC system in line with an LTQ-Orbitrap Velos mass spectrometer (Thermo Scientific). Peptides in 1% (v/v) formic acid were injected onto an Acclaim PepMap C18 nano-trap column (Thermo Scientific). After washing with 0.5% (v/v) acetonitrile, 0.1% (v/v) formic acid, peptides were resolved on a 250 mm × 75 µm Acclaim PepMap C18 reverse phase analytical column (Thermo Scientific) over a 150 min organic gradient, using 7 gradient segments (1-6% solvent B over 1 min, 6-15% solvent B over 58 min, 15-32% solvent B over 58 min, 32-40% solvent B over 5 min, 40-90% solvent B over 1 min, held at 90% solvent B for 6 min and then reduced to 1% solvent B over 1 min) with a flow rate of 300 nl min^{-1}. Solvent A was 0.1% formic acid and solvent B was aqueous 80% acetonitrile in 0.1% formic acid. Peptides were ionized by nano-electrospray ionization at 2.1 kV using a stainless steel emitter with an internal diameter of 30 µm (Thermo Scientific) and a capillary temperature of 250°C. Tandem mass spectra were acquired using an LTQ-Orbitrap Velos mass spectrometer controlled by Xcalibur 2.1 software (Thermo Scientific) and operated in data-dependent acquisition mode. The Orbitrap was set to analyse the survey scans at 60,000 resolution (at m/z 400) in the mass range m/z 300 to 2000 and the top ten multiply charged ions in each duty cycle selected for MS/MS in the LTQ linear ion trap. Charge state filtering, where unassigned precursor ions were not selected for fragmentation, and dynamic exclusion (repeat count, 1; repeat duration, 30s; exclusion list size, 500) were used. Fragmentation conditions in the LTQ were as follows: normalized collision energy, 40%; activation q, 0.25; activation time 10 ms; and minimum ion selection intensity, 500 counts.

The raw data files were processed and quantified using Proteome Discoverer software v1.2 (Thermo Scientific) and searched against the UniProt Human database plus appropriate APP sequences using the SEQUEST algorithm. Peptide precursor mass tolerance was set at 10ppm, and

MS/MS tolerance was set at 0.8 Da. Search criteria included carbamidomethylation of cysteine (+57.0214) as a fixed modification and oxidation of methionine (+15.9949) and appropriate SILAC labels ($^{2}H_4$-Lys, $^{13}C_6$-Arg for Medium and $^{13}C_6{}^{15}N_2$-Lys and $^{13}C_6{}^{15}N_4$-Arg for Heavy) as variable modifications. Searches were performed with full tryptic digestion and a maximum of 1 missed cleavage was allowed. The reverse database search option was enabled and all peptide data were filtered to satisfy false discovery rate of 5%. Protein ratios presented in Table 1 are averaged from two experimental repeats.

Bioinformatic analysis

Gene ontology analysis was performed with DAVID Bioinformatics Resources version 6.7 (available at http://david.abcc.ncifcrf.gov/ (Huang da *et al.* 2009a; Huang da *et al.* 2009b)) using UniProt accession numbers as identifiers. Manual curation was performed on the entire dataset to ensure recognition of UniProt identifiers by DAVID software.

RNA interference

Specific siRNAs for human GAP43 (Dharmacon, #L-011663-00-000 and Ambion, #4392420 ID s5569) and a non-targeting control siRNA (Dharmacon, #D-001810-10-05) were obtained. SH-SY5Y cells either untransfected or expressing APP695-FLAG or APP751-FLAG were seeded into 6-well plates at 500,000 cells per well and cultured overnight. Cells were washed with PBS and siRNA was delivered as a complex with DharmaFECT 1 (Dharmacon, #T-2001-04) at a final concentration of 50 nM. Cells were cultured for 48 h as described previously, before being washed once with PBS and cultured for a further 6 h, for APP-expressing cells, or for 24 h, for untransfected cells, in serum free Opti-MEM (Life Technologies, 11058021).

SDS-PAGE and western blot

Protein samples were separated by sodium dodecyl sulphate polyacrylamide gel electrophoresis (SDS-PAGE) on 7-17% acrylamide gradient gels. Proteins were then transferred to polyvinylidene difluoride membranes (Biorad, #1620177) and blocked for 1 h in PBS containing 0.1% Tween-20 (PBS-T) and 5% (w/v) skimmed milk powder. Membranes were incubated in primary antibody overnight at 4°C in PBS-T containing 2% (w/v) bovine serum albumin (BSA) (Sigma, #A2153) 22C11 (RRID: 11205566, 1:2000 mouse IgG, a kind gift from Dr James Duce, University of Leeds), anti-FLAG (1:1000 mouse IgG), anti-ataxin-10 (RRID:AB_2061167, 1:1000 rabbit IgG, Proteintech, #15693-1-AP), anti-GRP78 (RRID:AB_2119855, 1:1000 mouse IgG, Proteintech, #11587-1-AP), anti-14-3-3ζ/δ (1:1000, a kind gift from Prof. Stuart Pickering-Brown, University of Manchester), anti-Fe65 (RRID:AB_10562819, 1:1000 rabbit IgG, Abcam, #ab91650) and 1:10000 for anti-GAP43

(RRID:AB_1310252, 1:10000 rabbit IgG, Abcam, #ab75810) and anti-actin (RRID:AB_476744, 1:10000 mouse IgG, Sigma, #A5441). Membranes were subsequently washed three times in PBS-T then incubated in horseradish peroxidase-linked secondary antibodies in PBS-T containing 2% BSA for 1 h at room temperature. Membranes were then washed twice in PBS-T and finally in PBS. Membranes were incubated for 1 min in enhanced chemiluminescence western blotting substrate (Pierce, #10005943) and visualised using a Syngene Gbox XT4 (Syngene). Densitometric analysis was performed using Genetools software from Syngene. Molecular weight markers are indicated in kDa on the left-hand side of each blot.

Aβ and sAPP quantification

Aβ40 and Aβ42 were measured using the V-PLEX Aβ peptide panel 1 (6E10) assay (Meso Scale Discovery (MSD), #K15200E). sAPPα and sAPPβ were measured using the sAPPα/sAPPβ multiplex assay kit (MSD , #K15120E) according to the manufacturer's instructions. Assay plates were blocked and conditioned cell medium samples and standards buffered with 500 mM HEPES, pH 7.4 to a final concentration of 50 mM were loaded in duplicate. Following washing, and secondary antibody incubation, assays were read using the MESO QUICKPLEX SQ 120 and analysed using Meso Scale Discovery Workbench 4.0 software (MSD). The protein concentration of the conditioned medium was determined by BCA assay and sAPPα, sAPPβ and Aβ levels corrected for total protein concentration.

Data and Statistical analysis

Data were analysed as stated in the text and figure legends, and n numbers are specified. No randomisation and no blinding were performed for the analysis of this data. For statistical analysis, data were analysed using IBM SPSS Statistics 20 software. A normal distribution was assumed for all cell data as mean values were recorded from a population of cells (based on the assumption that cells from a clonal population will respond in a similar manner) and therefore parametric analyses were performed. Levene's test was first applied to all data to determine equality of variance between groups for comparison. For comparison between two data sets, an independent t-test was applied and the appropriate statistic determined depending on the equality of variance. For multiple comparison data were analysed using a one-way analysis of variance (ANOVA) with a Tukey post-hoc correction for multiple comparisons. A test for outliers was not necessary for analysis of these data. For all analyses, statistical significance was taken at $p<0.05$.

Results

Identification of the cellular interactome of APP isoforms

In order to identify the interactomes of the APP695 and APP751 isoforms, a C-terminal FLAG-tag was added to the proteins using standard gene cloning techniques. SH-SY5Y cells which endogenously express both the KPI and non-KPI APP isoforms were transfected with the cDNA encoding APP695-FLAG or APP751-FLAG, or with the vector only as a mock transfected control. The expression of APP was determined by immunoblot analysis with an anti-APP antibody, demonstrating the over-expression of the respective APP-tagged isoforms compared to the mock transfected cells, (Fig. 1A). Comparable expression of the two APP isoforms was achieved when corrected for endogenous APP in the mock transfected cell line (data not shown). Immunofluorescence microscopy of cells immunostained with anti-FLAG antibody indicated >75% of cells expressed the APP-FLAG constructs (Fig. 1B). Staining was largely perinuclear, overlapping with the marker TGN46, with some punctate staining also observed, consistent with APP being present mainly in the trans Golgi network and endocytic vesicles (Thinakaran & Koo 2008). Conditioned cell medium was subjected to a multiplex ELISA (Mesoscale Discovery V-PLEX Aβ peptide panel 1 or sAPPα/sAPPβ multiplex assay kit) to determine the amounts of sAPPα, sAPPβ and Aβ. Analysis showed significantly more sAPPα ($p=0.0002$) and sAPPβ ($p=0.0017$) in the conditioned cell medium from APP695-FLAG expressing cells compared to APP751-FLAG expressing cells (Fig. 1C). Concomitantly, significantly more Aβ40 ($p=0.0003$) and Aβ42 ($p=0.0002$) were present in the conditioned cell medium from APP695-FLAG expressing cells compared to the APP751-FLAG expressing cells (Fig. 1D). The ratio of Aβ42:Aβ40 was not significantly different when comparing APP695 and APP751 expressing cells (not shown). These data are in agreement with those previously reported with untagged forms of the APP isoforms (Belyaev *et al.* 2010).

To compare the cellular interactomes of APP695 and APP751 we employed a strategy where co-immunoprecipitation of APP was followed by quantitative proteomics (Fig. 2A). Cells stably expressing APP695-FLAG or APP751-FLAG, or the mock transfected cells, were SILAC labelled over a period of three weeks requiring >6 passages, ensuring sufficient amino acid labelling to allow discrimination between proteins immunoprecipitated specifically with APP from each sample. Following SILAC labelling and immunoprecipitation using anti-FLAG affinity gel, confirmation of the immunoprecipitation of APP and co-immunoprecipitation with Fe65, a well-known APP interactor (Ando *et al.* 2001), in the APP expressing cell lines was determined by immunoblot analysis (Fig. 2B). Reduced association of Fe65 was consistently observed in the bound fraction of the APP751 immunoprecipitations compared to the APP695 immunoprecipitations in multiple experimental repeats. Equal volumes of the bound fractions from the mock, APP695-FLAG and APP751-FLAG immunoprecipitations were then combined and proteins were identified and quantified using LC-MS/MS. 410 proteins were identified in both of two separate labelling, co-immunoprecipitation and mass spectrometry analyses.

This approach not only allows the identification of proteins specifically interacting with either of the APP isoforms, but also produces a quantitative interaction ratio giving insight into the extent to which each isoform interacts with a particular protein. Several parameters were set for the inclusion of an interactor in the final data set. The LC-MS/MS identification was carried out on two separate SILAC labelled immunoprecipitations and only proteins with peptide ratios calculated on the basis of at least 4 peptides over the two experiments were included in the analysis. Following removal of proteins which did not meet this criterion, the interaction ratios for each protein in the APP-expressing cell lines was compared to the mock expressing cell line for the remaining 297 proteins. The interaction ratios were Log2 converted and all of the proteins identified were plotted as a scatter plot (Fig. 3A). To determine whether proteins were specifically enriched in the immunoprecipitation samples from each APP cell line, all proteins whose interaction ratio did not exceed the average interaction ratio of the whole data set were removed, a method previously employed to determine the *in vivo* mouse brain interactome of APP (Kohli *et al.* 2012). Once Log2 converted this cut-off value for the APP695 interactome was 2.33 and for the APP751 interactome was 1.38 and represents a more conservative cut-off than the 2-fold (or 1 when Log2 converted) cut-off used in similar SILAC based interactome studies (Wu *et al.* 2012; Hosp *et al.* 2015). Enriched proteins, those considered to be significantly higher in abundance in the APP lines compared to the mock, were re-plotted (Fig. 3B), and are displayed in Table 1 along with peptide score (higher score represents higher quality data), peptide count (number of individual peptides used for quantification), sequence coverage for the two separate experiments, and binding ratios averaged from the two experiments. In validation of this method, immunoprecipitation of APP-FLAG and immunoblotting for proteins within the dataset (highlighted in Fig. 3B) showed that proteins in the interactome such as Fe65 were identifiable as enriched in immunoblots, while those excluded by the cut-offs were not (Fig. 3C). Indeed, while proteins such as 14-3-3ζ/δ were identified by mass spectrometry, they were not detectable by immunoblot as APP interactors and were removed by the cut-offs employed (Fig. 3C). Similarly, analysis of several other proteins which were removed by the cut offs employed, including NAP1L1, HSP27, HSP90, Karyopherin-β and Karyopherin-α were not detectable as enriched in the APP immunoprecipitations compared to control (data not shown). Final analysis revealed 36 proteins enriched in both the APP695 and APP751 interactome (Fig. 3D). In addition, 12 proteins were specifically enriched in the APP695 dataset and 22 were specifically enriched in the APP751 dataset (Fig. 3D).

Bioinformatics analysis

Gene ontology analysis of the APP interactome datasets showed enrichment of proteins involved in the nuclear pore and in nuclear transport in the APP695 interactome but not in the APP751 interactome (Table 2). Indeed, when just proteins interacting >2-fold more with APP695 than APP751

were subjected to gene ontology analysis, proteins involved in nuclear import remained significantly enriched (Table 3). Bioinformatic analysis also indicated enrichment of mitochondrial proteins in the APP695 interactome compared to that of APP751 (Table 2). As with nuclear proteins, enrichment of mitochondrial proteins was also seen when proteins interacting >2-fold higher with APP695 than with APP751 were analysed (Table 3).

Validation of interaction partners

To confirm the interaction of APP with some of the proteins identified in the mass spectrometry dataset, immunoprecipitations were carried out on APP695-FLAG, APP751-FLAG and mock transfected cell lines and the resulting bound fractions subjected to immunoblot analysis for GRP78, ITM2C, ataxin-10 and GAP43 that had been identified in the interactomes (Fig. 3E). Co-immunoprecipitation with both APP695 and APP751 was confirmed for GRP78. Ataxin-10 and ITM2C were preferentially co-immunoprecipitated with APP695, while GAP43 was preferentially co-immunoprecipitated with APP751, confirming the differential interactions identified in the mass spectrometry analysis. In some cases, residual protein remained in the bound fraction from the mock-transfected cell line, but consistently higher levels of the target protein were observed in the bound fractions for the APP isoform which the unbiased LC-MS/MS identified as an interactor.

GAP43 modulates APP751 proteolysis

Initially, to confirm the interaction between APP751 and GAP43, the reverse immunoprecipitation was carried out in APP751-FLAG transfected cells with the anti-GAP43 antibody and immunoblotting with the anti-APP antibody 22C11 (Fig. 4A). To rule out the interaction being a result of overexpression of APP751, we confirmed the co-immunoprecipitation of GAP43 with APP751 in untransfected SH-SY5Ycells which endogenously express both proteins (Fig. 4B). Finally, we investigated whether modulation of GAP43 altered APP processing firstly by using siRNA knockdown of GAP43 in SH-SY5Y cells expressing APP751-FLAG. GAP43 was knocked down by approximately 40% following siRNA treatment (Fig. 4C and 4D). In SH-SY5Y cells expressing APP695-FLAG there was no change in Aβ40 or Aβ42 but in SH-SY5Y cells expressing APP751-FLAG Aβ42 was significantly reduced upon knockdown of GAP43, by 26.2% ($p=0.0077$) (Fig. 4E). Aβ40 was also decreased, by 22.4%, but this was not significant (Fig. 4E). To f investigate the effect of GAP43 on APP proteolysis in untransfected SH-SY5Y cells we used siRNA knockdown of GAP43. Knockdown of GAP43 (by 67.6%, $p=0.0052$) was confirmed by immunoblot (Fig. 5A). Knockdown of GAP43 resulted in a significant reduction in sAPPα and sAPPβ, by 10.3% and 11.5% ($p=0.0247$ and $p=0.0217$), respectively (Fig. 5B) and in Aβ40 and Aβ42, by 18.1% and 23.4% ($p=0.0112$ and $p=0.0402$) respectively (Fig. 5C) compared to non-targeting control.

Discussion

The study of APP proteolysis within human cells has provided invaluable insights into the mechanisms involved in the production of Aβ. However, the cellular interactome of APP has not been widely studied and could increase understanding of the cellular interactions which influence its proteolysis. To this end we sought to elucidate the interactomes in a human neuronal cell line of the two most abundant APP isoforms in the human brain, namely APP695 and APP751, which are differentially processed by the β-secretase BACE1 to produce Aβ and the transcriptionally active AICD.

We used an unbiased mass spectrometry screening approach to identify proteins that interact with APP in cell culture. We identified 70 proteins which meet the criteria we have used to determine whether proteins are true interactors or not. These parameters are of course arbitrary, but we believe represent a stringent enough cut-off to identify only proteins which are direct interactors. Through the use of C-terminally FLAG-tagged APP constructs we have avoided the use of any anti-APP antibodies for the immunoprecipitation, the immunoreactivity of which may be blocked by interacting partners. Furthermore, we have shown that the addition of this 8 amino acid tag sequence does not affect the differential proteolysis of the APP isoforms previously described (Belyaev *et al.* 2010). Our experimental design, using C-terminally tagged APP constructs means that identified proteins may interact with full length APP, CTFs produced by α- or β-secretase proteolysis (C83 and C99, respectively), AICD or any other C-terminal containing fragment.

We used the well-studied interaction between APP and Fe65 to confirm the successful co-immunoprecipitation of a known APP interactor in the lysis conditions employed prior to the mass spectrometry analyses. This demonstrated the interaction of Fe65 with both APP isoforms to different extents, with a reduced association of Fe65 with the APP751 isoform compared to the APP695 isoform. The differential association of Fe65 with the different APP isoforms was later confirmed in the mass spectrometry analyses and is consistent with the differences in subsequent roles for these isoforms in transcriptional regulation that have been previously reported (Belyaev *et al.* 2010). Our dataset identified several proteins previously identified as APP interactors in mass spectrometry based studies in other model systems including Calnexin and HSPA5 (Bai *et al.* 2008), VDAC3 (Kohli *et al.* 2012; Hosp *et al.* 2015), ATP1A1 and SLC25A3 (Kohli *et al.* 2012). In addition, we were able to repeat the interactions identified in the mass spectrometry data using immunoprecipitation and western blot for five different interactors within the dataset. While high consensus in interactomic studies is often difficult to achieve (Perreau *et al.* 2010), different protein expression patterns in different cell types and *in vivo* make direct comparison inherently difficult.

Despite their well-studied roles in the proteolysis of APP, neither β- nor α-secretase was identified in the dataset, nor were any of the components of the γ-secretase complex. Another SILAC LC-MS/MS based analysis of APP interactors also failed to show co-immunoprecipitation of the

secretases, suggesting that the transient nature of their interaction may prevent their identification (Hosp *et al.* 2015). A comprehensive comparison of our dataset with the dataset of Hosp et al. 2015 recently published showed only one protein in that study met the cut off we set here for interaction (VDAC3). However, a further 16 were identified but did not make our final data set due to the stringent cut off criteria we employed. The differences in the interactions identified in our study and that of Hosp et al. may be due to the different cell lines (SH-SY5Y compared to HEK) and different positioning of the tag (C-terminus compared to N-terminus). The nuclear signalling capabilities of AICD appear to be specific to neuronal cells lines (Belyaev *et al.* 2010) suggesting specific interactions and trafficking pathways for APP and its metabolites may be restricted to neuronal cells. Interestingly, our dataset showed enrichment of proteins involved in nuclear transport, while that of Hosp et al. did not, supporting data suggesting trafficking of APP or fragments thereof to the nucleus is neuronal cell type specific (Belyaev *et al.* 2010).

The ontology analysis for our dataset showed enrichment of various mitochondrial proteins within the APP695 interactome. APP has previously been implicated in mitochondrial function and gene expression (Chua *et al.* 2013) and has been shown to accumulate in mitochondrial import channels in AD (Devi *et al.* 2006), while disruption of mitochondrial function has been widely reported in AD (Ankarcrona *et al.* 2010). The APP amino acid sequence contains a cryptic mitochondrial signal sequence suggesting that its presence in mitochondria is not solely due to aberrant localisation induced by over-expression (Anandatheerthavarada *et al.* 2003). Despite the fact that APP is orientated within the mitochondrial membrane with its N-terminus in the mitochondrial matrix and C-terminus in the cytosol, AICD has been shown to be present within the mitochondrial matrix (Pavlov *et al.* 2011). Given the postulated roles for AICD as a transcriptional regulator, it would be interesting to investigate whether this proteolytic APP fragment has a role in the regulation of mitochondrial genes. Indeed, this may explain the increased presence of mitochondrial proteins in this, and other, interactomic analyses of APP (Hosp *et al.* 2015). Hosp et al. investigated the interaction of APP with the protein LRPPRC, a key protein in mitochondrial gene regulation, which did appear in our data set when the arbitrary 2-fold cut off was employed, as was used in their study. While we also identified two proteins identified by Bai et al. in their *in vivo* interactome study, we did not observe interaction with Lingo-1, which the authors later showed modulated APP proteolysis (Bai et al. 2008). While our methodology allowed for interactions specific to a human cell type, they do not account for potential inter-cell interactions or interactions which may occur specifically in the highly-organised tissue of the brain. Additional proteins identified in our analysis may be present due to the use of a tagged APP construct, circumventing the requirement for the use of an anti-APP antibody, as used previously (Bai *et al.* 2008), the immunoreactivity of which could have been blocked by covalently linked interacting proteins in the C-terminal region of APP recognised by the antibody. Both our study and that of Bai et al. indicate that interrogation of the APP interactome may

aid in the identification of alternative mechanisms for disrupting APP proteolysis outside of direct secretase inhibition.

GAP43 was identified as interacting selectively with the APP751 isoform and in modulating its proteolysis by the secretases. GAP43 has previously been shown to localise with APP in presynaptic boutons in the frontal cortex of AD brains (Masliah *et al.* 1992b) and in outgrowing neurites of the neonatal rat brain (Masliah *et al.* 1992a). More recently, GAP43 has been identified as a potential biomarker for AD, with GAP43 measurements in cerebrospinal fluid shown to correlate with Aβ and tau (Sandelius *et al.* 2018). We demonstrate, for the first time that there is a direct interaction between GAP43 and the 751 isoform of APP, and that this interaction affects Aβ levels. Our data indicates that the interaction with GAP43 decreases both α- and β-secretase cleavage of APP751 as the respective secretase products sAPPα and sAPPβ are decreased upon GAP43 siRNA knockdown (Fig. 5B). It would appear that GAP43 also has an additional effect on γ-secretase as there was a greater decrease in Aβ levels than that seen in sAPPβ (Fig. 5C). GAP43 is a presynaptic protein (Wang *et al.* 2014), and the presynaptic membrane has previously been implicated as a site of BACE1 accumulation and amyloidogenic proteolysis of APP (DeBoer *et al.* 2014; Buggia-Prevot *et al.* 2014), while Aβ generation has also been shown to be activity-dependent in neurons (Kamenetz *et al.* 2003). Interaction with GAP43 may contribute to retention of APP within presynaptic regions, resulting in increased proteolysis of this APP isoform. GAP43 knockdown has previously been shown to reduce Aβ in the conditioned medium of HEK cells expressing APP, albeit using an APP695 construct. The decrease in Aβ was attributed to a direct interaction with the γ-secretase complex following the identification of GAP43 as a γ-secretase associated protein in human brain (Inoue *et al.* 2015). Our data indicates that GAP43 also directly interacts with APP751 and affects cleavage by both α- and β-secretase. However, as GAP43 does not influence APP695 processing, it cannot be exerting a direct effect on the secretases, but could be influencing access of APP751 to the secretases through preferential subcellular localisation, which could explain the differential proteolysis of the APP isoforms that was previously observed (Belyaev *et al.* 2010). As GAP43 is a cytosolic protein that attaches to the inside of the plasma membrane via palmitolyation, it cannot interact directly with the KPI domain in the extracellular domain of APP. As the cytosolic domains of APP695 and APP751 are identical in terms of protein sequence, the preferential interaction of APP751 with GAP43 may be due to colocalisation at the membrane, possibly within a subset of lipid rafts. However, it remains to be determined which protein is interacting selectively with the KPI domain to promote this distinct subcellular localisation of APP751.

In conclusion, our unbiased interactome screen has revealed a selective enrichment of proteins implicated in mitochondrial function, nuclear transport and the nuclear pore in the APP695 interactome in neuronal cells. This provides further evidence for a preferential role of APP695, rather than APP751, in transcriptional regulation and mitochondrial function and/or dysfunction. In addition,

we have identified various proteins that interact selectively with either APP695 or APP751. Finally, we have shown that a novel direct binding partner (GAP43) selectively influences the proteolytic processing of APP751.

Author contribution

RJA, KABK and NMH designed the study. RJA, KF, KABK and KJH performed the research. RJA, KF, KABK and NMH analysed data. RJA, KABK and NMH wrote the paper. All authors have given approval to the final version of the manuscript.

Acknowledgements and conflict of interest disclosure

We gratefully acknowledge the financial support of Alzheimer's Research UK (PhD2012-5 and PG2013-12), the University of Leeds, the University of Manchester and the Dr Donald Dean Fund for Dementia Research. The Bioimaging Facility microscopes used in this study were purchased with grants from BBSRC, Wellcome and the University of Manchester Strategic Fund. We thank H. Jarosz-Griffiths and B. Allsop (University of Manchester) for their help with the microscopy. The authors have no conflict of interest to declare.

References

Anandatheerthavarada, H. K., Biswas, G., Robin, M. A. and Avadhani, N. G. (2003) Mitochondrial targeting and a novel transmembrane arrest of Alzheimer's amyloid precursor protein impairs mitochondrial function in neuronal cells. *J Cell Biol* **161,** 41-54.

Ando, K., Iijima, K. I., Elliott, J. I., Kirino, Y. and Suzuki, T. (2001) Phosphorylation-dependent regulation of the interaction of amyloid precursor protein with Fe65 affects the production of beta-amyloid. *J Biol Chem* **276,** 40353-40361.

Andrew, R. J., Kellett, K. A., Thinakaran, G. and Hooper, N. M. (2016) A Greek Tragedy: the Growing Complexity of Alzheimer Amyloid Precursor Protein Proteolysis. *J Biol Chem* **291,** 19235-19244.

Ankarcrona, M., Mangialasche, F. and Winblad, B. (2010) Rethinking Alzheimer's disease therapy: are mitochondria the key? *J Alzheimers Dis* **20 Suppl 2,** S579-590.

Bai, Y., Markham, K., Chen, F. et al. (2008) The in Vivo Brain Interactome of the Amyloid Precursor Protein. *Mol Cell Proteomics* **7,** 15-34.

Belyaev, N. D., Kellett, K. A., Beckett, C., Makova, N. Z., Revett, T. J., Nalivaeva, N. N., Hooper, N. M. and Turner, A. J. (2010) The transcriptionally active amyloid precursor protein (APP) intracellular domain is preferentially produced from the 695 isoform of APP in a β-secretase-dependent pathway. *J Biol Chem* **285,** 41443-41454.

Buggia-Prevot, V., Fernandez, C. G., Riordan, S., Vetrivel, K. S., Roseman, J., Waters, J., Bindokas, V. P., Vassar, R. and Thinakaran, G. (2014) Axonal BACE1 dynamics and targeting in hippocampal neurons: a role for Rab11 GTPase. *Mol Neurodegener* **9,** 1.

Chua, L. M., Lim, M. L. and Wong, B. S. (2013) The Kunitz-protease inhibitor domain in amyloid precursor protein reduces cellular mitochondrial enzymes expression and function. *Biochem Biophys Res Commun* **437,** 642-647.

Cottrell, B. A., Galvan, V., Banwait, S. et al. (2005) A pilot proteomic study of amyloid precursor interactors in Alzheimer's disease. *Ann Neurol* **58,** 277-289.

De Strooper, B. and Karran, E. (2016) The Cellular Phase of Alzheimer's Disease. *Cell* **164,** 603-615.

DeBoer, S. R., Dolios, G., Wang, R. and Sisodia, S. S. (2014) Differential release of beta-amyloid from dendrite- versus axon-targeted APP. *J Neurosci* **34,** 12313-12327.

Devi, L., Prabhu, B. M., Galati, D. F., Avadhani, N. G. and Anandatheerthavarada, H. K. (2006) Accumulation of amyloid precursor protein in the mitochondrial import channels of human Alzheimer's disease brain is associated with mitochondrial dysfunction. *J Neurosci* **26,** 9057-9068.

Golde, T. E., Estus, S., Usiak, M., Younkin, L. H. and Younkin, S. G. (1990) Expression of beta amyloid protein precursor mRNAs: recognition of a novel alternatively spliced form and quantitation in Alzheimer's disease using PCR. *Neuron* **4,** 253-267.

Grimm, M. O., Mett, J., Stahlmann, C. P. et al. (2015) APP intracellular domain derived from amyloidogenic beta- and gamma-secretase cleavage regulates neprilysin expression. *Front Aging Neurosci* **7,** 77.

Haass, C., Kaether, C., Thinakaran, G. and Sisodia, S. (2012) Trafficking and Proteolytic Processing of APP. *Cold Spring Harb Perspect Med* **2,** a006270.

He, W., Lu, Y., Qahwash, I., Hu, X. Y., Chang, A. and Yan, R. (2004) Reticulon family members modulate BACE1 activity and amyloid-beta peptide generation. *Nat Med* **10,** 959-965.

Hosp, F., Vossfeldt, H., Heinig, M. et al. (2015) Quantitative interaction proteomics of neurodegenerative disease proteins. *Cell Rep* **11,** 1134-1146.

Huang da, W., Sherman, B. T. and Lempicki, R. A. (2009a) Bioinformatics enrichment tools: paths toward the comprehensive functional analysis of large gene lists. *Nucleic Acids Res* **37,** 1-13.

Huang da, W., Sherman, B. T. and Lempicki, R. A. (2009b) Systematic and integrative analysis of large gene lists using DAVID bioinformatics resources. *Nat Protoc* **4,** 44-57.

Inoue, M., Hur, J. Y., Kihara, T. et al. (2015) Human brain proteins showing neuron-specific interactions with gamma-secretase. *FEBS J* **282,** 2587-2599.

Kamenetz, F., Tomita, T., Hsieh, H., Seabrook, G., Borchelt, D., Iwatsubo, T., Sisodia, S. and Malinow, R. (2003) APP processing and synaptic function. *Neuron* **37,** 925-937.

Kohli, B. M., Pflieger, D., Mueller, L. N., Carbonetti, G., Aebersold, R., Nitsch, R. M. and Konietzko, U. (2012) Interactome of the amyloid precursor protein APP in brain reveals a protein network involved in synaptic vesicle turnover and a close association with Synaptotagmin-1. *J Proteome Res* **11,** 4075-4090.

Masliah, E., Mallory, M., Ge, N. and Saitoh, T. (1992a) Amyloid precursor protein is localized in growing neurites of neonatal rat brain. *Brain Res* **593,** 323-328.

Masliah, E., Mallory, M., Hansen, L., Alford, M., DeTeresa, R., Terry, R., Baudier, J. and Saitoh, T. (1992b) Localization of amyloid precursor protein in GAP43-immunoreactive aberrant sprouting neurites in Alzheimer's disease. *Brain Res* **574,** 312-316.

Masters, C. L., Simms, G., Weinman, N. A., Multhaup, G., McDonald, B. L. and Beyreuther, K. (1985) Amyloid plaque core protein in Alzheimer disease and Down syndrome. *Proc. Natl. Acad. Sci. USA* **82,** 4245-4249.

Matsui, T., Ingelsson, M., Fukumoto, H., Ramasamy, K., Kowa, H., Frosch, M. P., Irizarry, M. C. and Hyman, B. T. (2007) Expression of APP pathway mRNAs and proteins in Alzheimer's disease. *Brain Res* **1161,** 116-123.

Moir, R. D., Lynch, T., Bush, A. I. et al. (1998) Relative increase in Alzheimer's disease of soluble forms of cerebral Ab amyloid protein precursor containing the kunitz protease inhibitory domain. *J. Biol. Chem.* **273,** 5013-5019.

Munday, D. C., Surtees, R., Emmott, E., Dove, B. K., Digard, P., Barr, J. N., Whitehouse, A., Matthews, D. and Hiscox, J. A. (2012) Using SILAC and quantitative proteomics to investigate the interactions between viral and host proteomes. *Proteomics* **12,** 666-672.

Pardossi-Piquard, R., Petit, A., Kawarai, T. et al. (2005) Presenilin-Dependent Transcriptional Control of the Aβ-Degrading Enzyme Neprilysin by Intracellular Domains of βAPP and APLP. *Neuron* **46,** 541-554.

Pavlov, P. F., Wiehager, B., Sakai, J., Frykman, S., Behbahani, H., Winblad, B. and Ankarcrona, M. (2011) Mitochondrial gamma-secretase participates in the metabolism of mitochondria-associated amyloid precursor protein. *FASEB J* **25,** 78-88.

Perreau, V. M., Orchard, S., Adlard, P. A. et al. (2010) A domain level interaction network of amyloid precursor protein and Abeta of Alzheimer's disease. *Proteomics* **10,** 2377-2395.

Reinhard, C., Hebert, S. S. and De Strooper, B. (2005) The amyloid-β precursor protein: integrating structure with biological function. *EMBO J.* **24,** 3996-4006.

Rice, H. C., Young-Pearse, T. L. and Selkoe, D. J. (2013) Systematic evaluation of candidate ligands regulating ectodomain shedding of amyloid precursor protein. *Biochemistry* **52,** 3264-3277.

Sandbrink, R., Masters, C. L. and Beyreuther, K. (1996) APP gene family. Alternative splicing generates functionally related isoforms. *Ann N Y Acad Sci* **777,** 281-287.

Sandelius, A., Portelius, E., Kallen, A. et al. (2018) Elevated CSF GAP-43 is Alzheimer's disease specific and associated with tau and amyloid pathology. *Alzheimers dement*.

Soba, P., Eggert, S., Wagner, K. et al. (2005) Homo- and heterodimerization of APP family members promotes intercellular adhesion. *EMBO J.* **24,** 3624-3634.

Thinakaran, G. and Koo, E. H. (2008) Amyloid Precursor Protein Trafficking, Processing, and Function. *J Biol Chem* **283,** 29615-29619.

Wakabayashi, T., Craessaerts, K., Bammens, L. et al. (2009) Analysis of the γ-secretase interactome and validation of its association with tetraspanin-enriched microdomains. *Nat Cell Biol* **11,** 1340-1346.

Wang, H., Wang, R., Xu, S. and Lakshmana, M. K. (2014) RanBP9 overexpression accelerates loss of pre and postsynaptic proteins in the APDeltaE9 transgenic mouse brain. *PLoS ONE* **9,** e85484.

Wang, Z., Wang, B., Yang, L., Guo, Q., Aithmitti, N., Songyang, Z. and Zheng, H. (2009) Presynaptic and postsynaptic interaction of the amyloid precursor protein promotes peripheral and central synaptogenesis. *J Neurosci* **29,** 10788-10801.

Wu, W., Tran, K. C., Teng, M. N., Heesom, K. J., Matthews, D. A., Barr, J. N. and Hiscox, J. A. (2012) The interactome of the human respiratory syncytial virus NS1 protein highlights multiple effects on host cell biology. *J Virol* **86,** 7777-7789.

Uniprot Accession	Gene name	Score Expt 1 /Expt 2	Peptide Expt 1 /Expt 2	Coverage Expt 1/ Expt 2 (%)	APP695:Control ratio		APP751:Control ratio		APP695:APP751 ratio	
					Binding ratio	Peptide	Binding ratio	Peptide	Binding ratio	Peptide
Q5JTZ9	***AARS2***	7.2/24.1	2/4	2.4/5.6	100.00	4	1.00	4	71.41	6
O00213	APBB1	19.0/42.8	4/6	10.4/12.7	100.00	10	7.55	11	61.67	10
Q9UBX3	***SLC25A10***	9.4/24.5	1/2	3.5/8.7	75.71	4	1.22	4	60.55	5
Q9UBB4	ATXN10	11.7/14.9	3/2	8.2/6.1	63.03	5	2.94	5	60.52	5
P08183	***ABCB1***	27.8/7.8	4/1	4.0/1.2	38.03	3	2.22	3	21.78	5
O43592	XPOT	15.3/20.0	3/3	4.0/4.0	35.21	3	2.72	3	19.99	5
Q92870	APBB2	32.6/49.8	3/3	4.4/10.7	12.00	9	79.59	10	11.12	9
P55060	***CSE1L***	32.4/35.3	6/5	7.6/11.8	64.53	8	1.82	8	8.27	11
O95373	***IPO7***	13.4/44.3	4/6	5.1/8.3	13.95	8	2.19	8	6.92	10
Q9H9B4	SFXN1	11.2/32.5	2/7	7.1/21.4	26.31	5	3.45	5	4.74	8
P53985	SLC16A1	11.1/22	2/3	6.7/7.3	15.16	4	4.33	4	4.67	5
O00483	NDUFA4	5.1/19	2/3	27.1/37.0	9.33	5	2.74	5	4.60	5
Q92973	TNPO1	16.5/15.9	3/2	3.9/2.8	9.21	5	2.80	5	4.17	5
P55084	***HADHB***	38.17/15	6/3	13.7/7.8	7.84	6	2.19	5	3.98	7
O75473	***LRG5***	37.6/8.4	5/1	7.0/1.4	36.49	5	2.00	5	2.47	8
E1NZA1	PRIC295	33.8/93.5	7/18	2.8/9.3	30.41	14	3.54	14	2.33	22
O14980	XPO1	9.8/54.6	2/7	3.3/8.7	13.06	8	4.65	8	1.99	9
P12236	SLC25A6	78.8/135.7	7/9	24.5/27.2	22.66	7	5.68	7	1.98	10
P36542	***ATP5C1***	15.0/16.6	3/4	13.6/31.5	11.00	8	1.88	8	1.96	8
P78527	PRKDC	142.7/309.7	23/48	6.8/13.7	12.11	50	4.54	50	1.92	66
Q9ULH0	KIDINS220	32.6/8.8	5/1	3.3/1.0	8.92	7	4.18	7	1.89	7
P16615	***ATP2A2***	28.2/87.0	4/11	4.8/13.0	28.95	14	2.38	14	1.88	17
P05141	SLC25A5	94.9/131.2	8/9	27.9/25.5	6.64	10	3.71	10	1.79	12
O43175	***PHGDH***	26.4/23.2	6/5	13.4/11.8	7.89	6	2.30	6	1.70	10
P31689	DNAJA1	32.6/71.7	8/7	20.9/22.7	8.34	13	3.56	12	1.64	15
Q9UJS0	SLC25A13	76.8/142.0	9/14	18.5/27.6	7.92	19	4.67	20	1.63	28
Q53H12	**AGK**	**13.3/3.4**	**3/1**	**8.6/5.3**	**4.57**	**4**	**2.83**	**4**	**1.59**	**4**
Q9NQX7	ITM2C	59.9/13.1	7/2	31.8/18.3	52.68	11	2.64	11	1.59	15
P53007	***SLC25A1***	6.4/28.1	1/3	5.8/11.3	100.00	1	1.00	1	1.56	5
P25705	**ATP5A1**	**69.5/106.49**	**8/12**	**18.8/26.8**	**4.35**	**25**	**2.83**	**25**	**1.53**	**27**
P57088	SHINC3	5.8/40.2	2/5	9.9/18.2	6.29	6	17.77	7	1.52	7
Q15758	***SLC1A5***	15.1/28.4	2/4	3.9/10.9	8.37	7	2.55	7	1.50	8
O60762	DPM1	13.9/29.5	2/5	10.6/31.8	6.93	6	4.98	6	1.48	9
P02786	**TFRC**	**52.5/19.8**	**8/3**	**12.2/5.7**	**4.97**	**10**	**3.65**	**10**	**1.48**	**11**
Q96HS1	PGAM5	104.3/152.4	4/8	12.5/31.5	19.01	26	11.42	26	1.46	30
P04843	RPN1	71.3/92.3	6/11	13.6/26.8	5.74	19	3.57	19	1.46	23
Q96AY4	TTC28	12.5/18.6	1/3	0.5/1.4	6.75	2	5.20	2	1.46	4
O14828	SCAMP3	17.5/42.7	2/3	8.4/14.1	5.92	6	4.05	6	1.46	7
P68363	TUBA1B	171.0/477.9	12/17	38.9/56.5	5.61	5	3.87	5	1.45	5
Q71U36	TUBA1A	177.6/479.0	12/17	38.9/56.5	7.19	5	3.63	5	1.45	5
P43307	SSR1	6.7/11.3	2/2	7.2/9.8	5.40	2	3.37	2	1.40	4
Q9Y277	**VDAC3**	**10.7/10.3**	**3/2**	**14.5/7.4**	**3.68**	**4**	**2.73**	**4**	**1.38**	**4**
P56134	ATP5J2	9.8/26.4	2/2	49.0/49.0	5.35	6	3.97	6	1.37	6
A6NKG5	RTL1	29.2/140.5	5/16	4.0/16	5.28	18	3.70	18	1.35	23
P27708	CAD	16.8/32.3	2/3	1.2/1.9	5.89	4	3.59	9	1.33	5
P62491	**RAB11A**	**19.2/15.9**	**3/2**	**22.6/15.5**	**3.07**	**5**	**2.72**	**4**	**1.31**	**6**
P50416	CPT1A	14.5/31.0	2/3	3.4/5.2	11.02	3	8.37	5	1.30	5
P05023	ATP1A1	75.8/67.5	10/8	13.6/11.1	8.12	6	6.20	3	1.29	10
P04792	**HSPB1**	**30.5/53.2**	**4/4**	**23.4/25.9**	**4.72**	**9**	**4.02**	**6**	**1.27**	**11**
Q00325	SLC25A3	46.8/67.6	2/4	8.6/21.3	7.14	11	4.04	9	1.22	12
Q16891	**IMMT**	**65.0/86.23**	**6/9**	**15.3/17.0**	**4.23**	**10**	**13.24**	**12**	**1.22**	**11**
Q13409	DYNC1I2	24.2/11.8	3/1	16.1/19.1	6.66	4	6.18	4	1.19	5
P39656	**DDOST**	**18.6/25.6**	**3/3**	**7.5/10.5**	**4.25**	**6**	**8.47**	**6**	**1.15**	**7**
P40939	**HADHA**	**35.6/48.4**	**6/7**	**9.5/13.5**	**4.21**	**12**	**3.46**	**12**	**1.14**	**13**
P08195	**SLC3A2**	**15.8/30.0**	**2/2**	**5.3/5.1**	**3.05**	**4**	**2.74**	**4**	**1.13**	**4**
P53618	**COPB1**	**14.2/28.1**	**3/3**	**8.4/5.4**	**2.88**	**4**	**3.37**	**4**	**1.08**	**5**
Q96N67	**DOCK7**	**20.7/23.1**	**4/3**	**2.3/2.0**	**2.49**	**6**	**3.37**	**6**	**1.07**	**7**
P53621	**COPA**	**40.8/21.1**	**7/3**	**7.3/3.4**	**3.02**	**8**	**2.93**	**9**	**1.04**	**10**
P27824	**CANX**	**35.3/35.1**	**3/5**	**9.1/10.0**	**3.21**	**8**	**3.49**	**8**	**1.04**	**9**
Q92504	SLC39A7	15.0/26.0	1/1	3.7/3.7	9.47	6	8.09	6	1.03	7
Q9NR30	DDX21	10.1/25.3	1/3	1.4/4.7	25.89	4	25.87	55	1.02	4
P11021	**HSPA5**	**310.3/272.1**	**23/25**	**40.2/41.1**	**3.96**	**55**	**4.45**	**5**	**0.87**	**62**
P61026	**RAB10**	**24.2/54.0**	**3/4**	**17.0/22.5**	**2.91**	**5**	**3.34**	**11**	**0.83**	**6**
P09172	**DBH**	**5.4/92.8**	**1/13**	**1.6/24.3**	**2.66**	**11**	**3.63**	**4**	**0.82**	**15**
Q09028	**RBBP4**	**25.9/6.88**	**5/1**	**18.1/3.8**	**1.23**	**5**	**2.80**	**13**	**0.81**	**4**
P49411	**TUFM**	**40.1/71.9**	**3/9**	**9.3/27.2**	**2.66**	**14**	**3.18**	**4**	**0.77**	**14**
O95831	AIFM1	5.8/11.6	2/3	11.5/6.4	13.71	3	8.33	4	0.71	4
Q9UHL4	**DPP7**	**9.88/26.6**	**2/3**	**6.7/8.5**	**1.08**	**4**	**6.46**	**13**	**0.39**	**4**
Q06830	**PRDX1**	**20.25/72.22**	**3/7**	**21.6/51.3**	**0.85**	**13**	**2.63**	**4**	**0.35**	**13**
P17677	**GAP43**	**9.1/34.7**	**1/2**	**9.7/16.4**	**0.84**	**4**	**3.74**	**10**	**0.23**	**4**

Table 1 - The APP695 and APP751 interactomes

A comprehensive list of all proteins identified as enriched in the APP isoform interactomes across the two experiments including details of the Uniprot identifier (http://www.uniprot.org) used for subsequent ontology analyses and gene name. Peptide score, peptide count and sequence coverage are shown from each of the two experiments, as well as the average interaction ratio from the two experiments comparing all three experimental cell lines. Lines in bold font indicate proteins determined to be APP751 specific and in those in bold/italic font were determined to be APP695 specific using the cut-off criteria employed. Protein sequences are available at UniProt.

Interactome	Category	Function term	Uniprot ID	Fold enrichment	P-value (Benjamini)
APP695	Biological process	ATP biosynthetic pathway	P56134, P05023, P36542, P16615, Q9UJS0	18.1	$1.6x10^{-2}$
APP695	Biological process	Nuclear transport	O95373, Q92973, P55060, O14980, O43592	10.2	$3.2x10^{-2}$
APP695	Cellular component	Nuclear pore	O95373, Q92973, P55060, O14980, O43592	18.4	$1.9x10^{-3}$
APP751	Cellular component	Cytoplasmic membrane-bounded vesicle	P27824, P09172, P02786, P05067, P62491, P53621, P08195, P04843, Q9UHL4, P11021, P57088, P05023, Q06830, P53618	5.8	$7.91x10^{-6}$

Table 2- Gene ontology analysis of APP isoform interacting proteins

The interactomes of the APP isoforms were subject to gene ontology analysis to identify functions enriched in their interactomes. Gene ontology analysis was performed on proteins that were considered to be enriched in each APP isoform interactome. Uniprot accession numbers were used as gene identifiers and ontology analysis carried out using DAVID software (http://david.abcc.ncifcrf.gov/).

Category	Function term	Uniprot ID	Fold enrichment	P-value
Biological process	Protein import into nucleus, docking	O95373, Q92973, P55060	159.2	$3.9x10^{-2}$
Cellular component	Mitochondrial part	O95373, Q92973, P55060, O43592	7.1	$4.4x10^{-2}$

Table 3- Mitochondrial and nuclear proteins are enriched in the APP695 interactome

Further gene ontology analysis was performed on proteins which showed large differences in interaction ratio between isoforms. Proteins which showed at least 2-fold higher interaction with either isoform were analysed using DAVID software.

FIGURE LEGENDS

Fig. 1: Expression and proteolysis of FLAG-tagged APP constructs

A) SH-SY5Y cells stably expressing APP695-FLAG or APP751-FLAG in the vector pIREShyg, or mock transfected cells expressing vector only were lysed and subjected to immunoblot analysis for APP and actin. Unglycosylated forms of both APP695 and APP751 (imm695, imm751) and glycosylated forms (m695, m751) are observed. **B)** Immunofluorescent microscopy of APP695-FLAG or APP751-FLAG expressing cells and their subcellular localisation in relation to the trans-Golgi network marker TGN-46. Immunofluorescence for both APP isoforms, using an anti-FLAG antibody, overlapped with that of TGN46, a trans-Golgi network marker (Yellow arrows) and showed punctate staining within the cell (white arrows). Scale bar = 10μm. ELISA analysis of **C)** sAPPα and sAPPβ and **D)** Aβ40 and Aβ42 in the conditioned cell medium from APP695-FLAG and APP751-FLAG expressing cells, corrected for the amount observed in the conditioned cell medium from mock transfected cells. Data are taken from three independent cell culture experiments, n= 3 samples per group, and are shown as mean ± S.E.M. **p<0.01, ***p<0.001 for APP751 compared to APP695.

Fig. 2: The experimental strategy for the identification of the APP interactome

A) Schematic representation of the SILAC LC-MS/MS strategy. SH-SY5Y cells expressing APP695-FLAG, APP751-FLAG or mock transfected cells were labelled by SILAC. FLAG-tagged APP was immunoprecipitated from cell lysates and analysis of the bound immunoprecipitation fractions was carried out by LC-MS/MS. **B)** Following SILAC, immunoprecipitation of FLAG-tagged proteins was performed using anti-FLAG affinity gel. Input (In), unbound (UB) and bound (B) fractions from the three immunoprecipitations were subjected to immunoblot analysis using anti-FLAG and anti-Fe65 antibody. * denotes non-specific bands.

Fig. 3: Identification of enriched data from mass spectrometry analysis and validation of interactors by co-immunoprecipitation

A) Protein interaction ratios from mass spectrometry analyses were Log2 converted and plotted as the ratio of APP695:mock against the ratio of APP751:mock. **B)** Cut-off values were determined and were Log2 converted giving cut-off values of 2.325 and 1.379 for the APP695 and APP751 interactomes, respectively. These cut-offs were applied to the data set to provide an enriched data set indicating specific interactors for each isoform. **C)** FLAG immunoprecipitations were performed on mock, APP695-FLAG and APP751-FLAG expressing cells and subjected to immunoblot for APP, Fe65, and 14-3-3 ζ/δ**.** * denotes non-specific bands. **D)** The cut-offs employed identified 36 proteins which interact with both APP isoforms. A further 12 proteins were identified which interacted specifically with APP695 and 22 which interacted specifically with APP751. **E)** Immunoprecpitations using anti-FLAG resin were performed on cell lysates from mock, APP695-FLAG and APP751-

FLAG expressing SH-SY5Y cells and bound fractions were immunoblotted for APP, ataxin-10, GRP78, ITM2C and GAP43.

Fig.4: GAP43 co-immunoprecipitates with APP751 and knockdown of GAP43 reduces Aβ in APP751-FLAG, but not APP695-FLAG expressing cells

Co-immunoprecipitation using anti-GAP43 antibody was performed on cell lysates from **A**) APP751 expressing SH-SY5Y cells and **B**) SH-SY5Y untransfected cells; bound fractions were immunoblotted for APP. * denotes non-specific bands. GAP43 was knocked down in **C)** APP695-FLAG expressing and **D)** APP751-FLAG expressing SH-SY5Y cells using 50nM smartpool siRNA complexed with DharmaFECT 1 transfection reagent in DMEM for 48 h. The cell medium was replaced with Opti-MEM and cells were cultured for a further 6 h. Cells were lysed and subjected to immunoblot analysis for APP, GAP43 and actin. **E)** ELISA analysis for Aβ40, and Aβ42 in the conditioned cell medium from APP695-FLAG and APP751-FLAG expressing cells. Aβ levels are shown as a percentage of the non-targeting control from the relevant cell line. Data are taken from three independent cell culture experiments, n= 3 samples per group, and are shown as mean ± S.E.M. **p-value <0.01.

Fig. 5: GAP43 siRNA knockdown decreases Aβ via alterations in the processing of APP751

GAP43 was knocked down in untransfected SH-SY5Y cells using 50nM siRNA (Ambion) complexed with DharmaFECT 1 transfection reagent in DMEM for 48 h. The cell medium was replaced with OPTIMEM and cells were cultured for a further 24 h. Cells were lysed and subjected to **A)** immunoblot analysis for GAP43, APP and actin in the lysates. Conditioned media was collected and analysed by ELISA for **B)** sAPPα and sAPPβ and **C)** Aβ40 and Aβ42 Data are taken from three independent cell culture experiments, n=3 samples per group, and are shown as mean ± S.E.M. *p-value <0.05 compared to control.

Figure 1

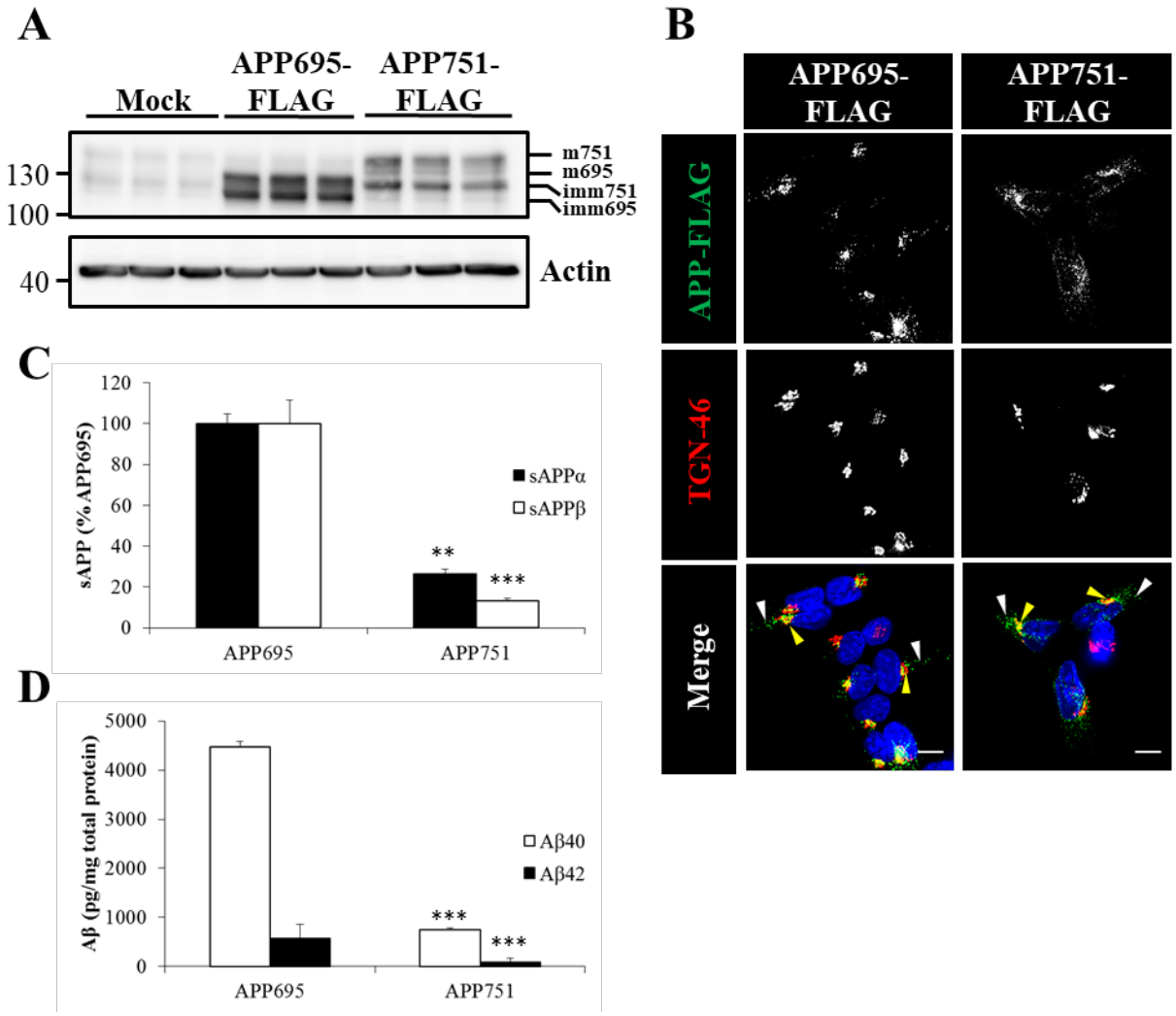
A
Mock
APP695-FLAG
APP751-FLAG
130
100
40
m751
m695
imm751
imm695
Actin
B
APP695-FLAG
APP751-FLAG
APP-FLAG
TGN-46
Merge
C
sAPP (% APP695)
120
100
80
60
40
20
0
sAPPα
sAPPβ
**
***
APP695
APP751
D
Aβ (pg/mg total protein)
5000
4000
3000
2000
1000
0
Aβ40
Aβ42
***
***
APP695
APP751

A

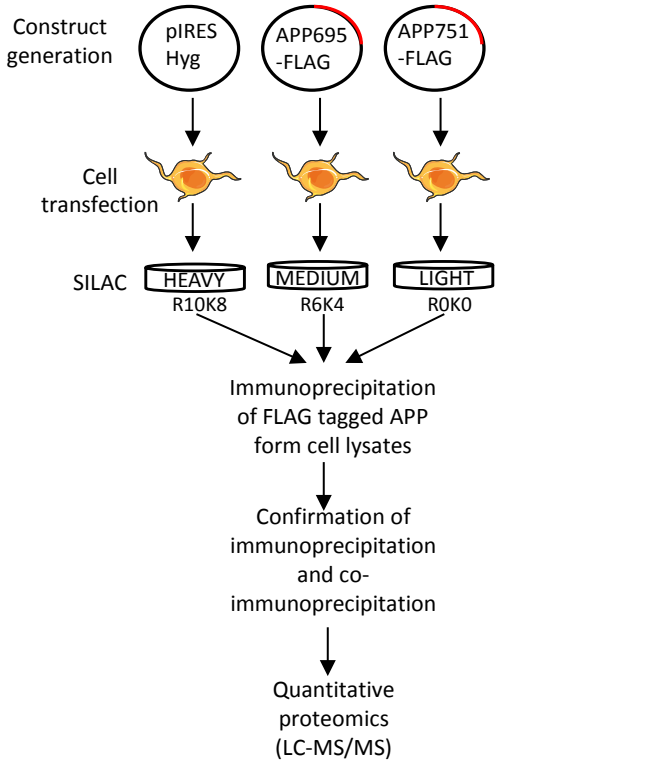
Construct generation
pIRES Hyg
APP695 -FLAG
APP751 -FLAG
Cell transfection
SILAC
HEAVY
R10K8
MEDIUM
R6K4
LIGHT
R0K0
Immunoprecipitation of FLAG tagged APP form cell lysates
Confirmation of immunoprecipitation and co-immunoprecipitation
Quantitative proteomics (LC-MS/MS)

B

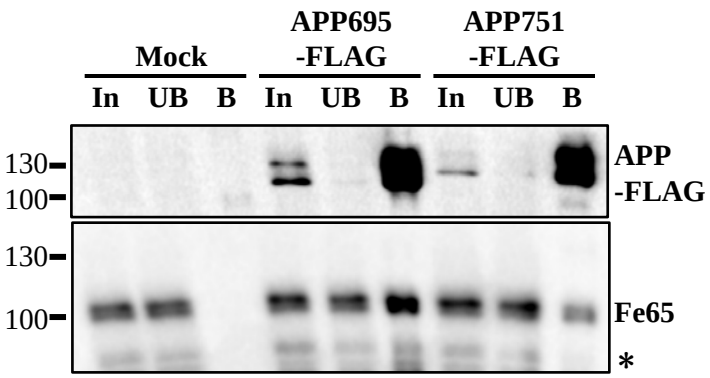
Mock
APP695 -FLAG
APP751 -FLAG
In UB B In UB B In UB B
130
100
APP -FLAG
130
100
Fe65
*

Figure 3

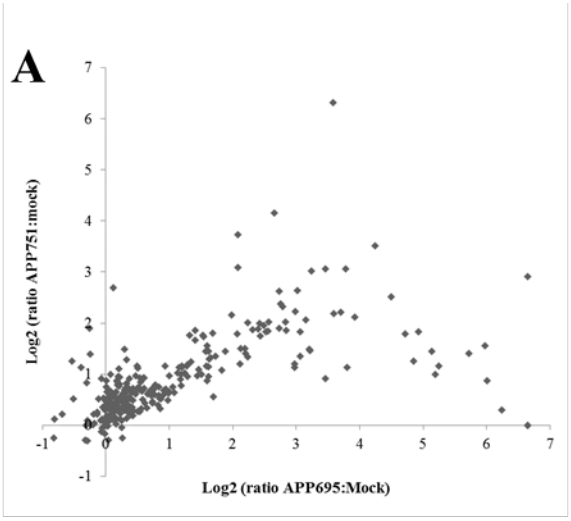
A
Log2 (ratio APP751:mock)
Log2 (ratio APP695:Mock)

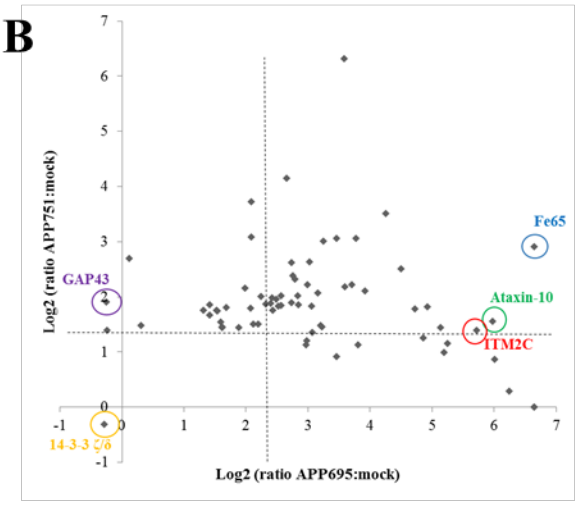
B
Log2 (ratio APP751:mock)
Log2 (ratio APP695:mock)
Fe65
GAP43
Ataxin-10
ITM2C
14-3-3 ζ/δ

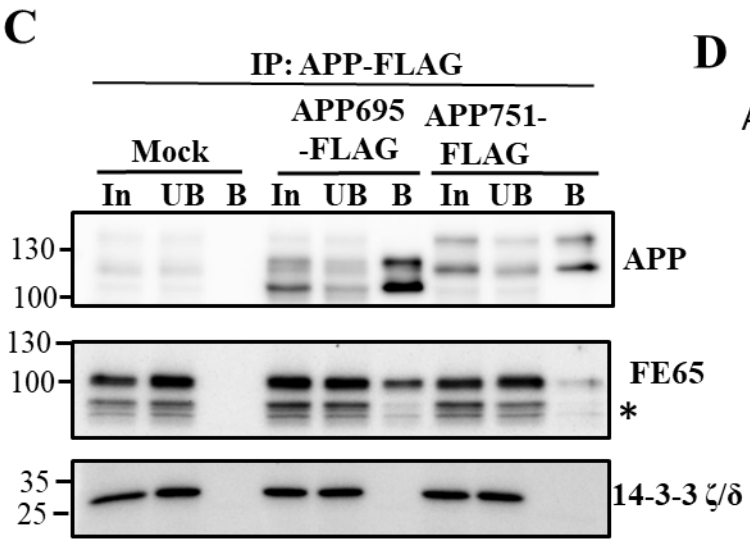
C
IP: APP-FLAG
Mock
APP695 -FLAG
APP751-FLAG
In UB B In UB B In UB B
130
100
APP
130
100
FE65
*
35
25
14-3-3 ζ/δ

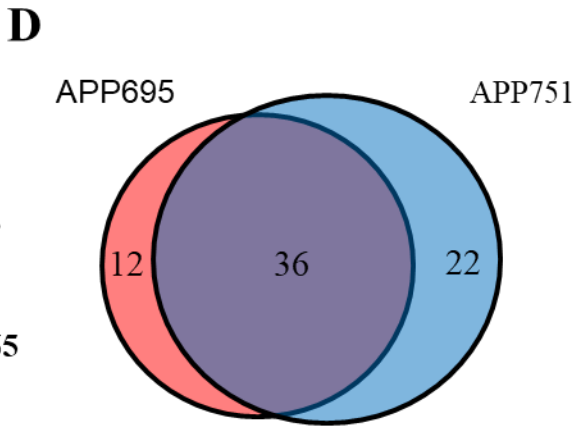
D
APP695
APP751
12
36
22

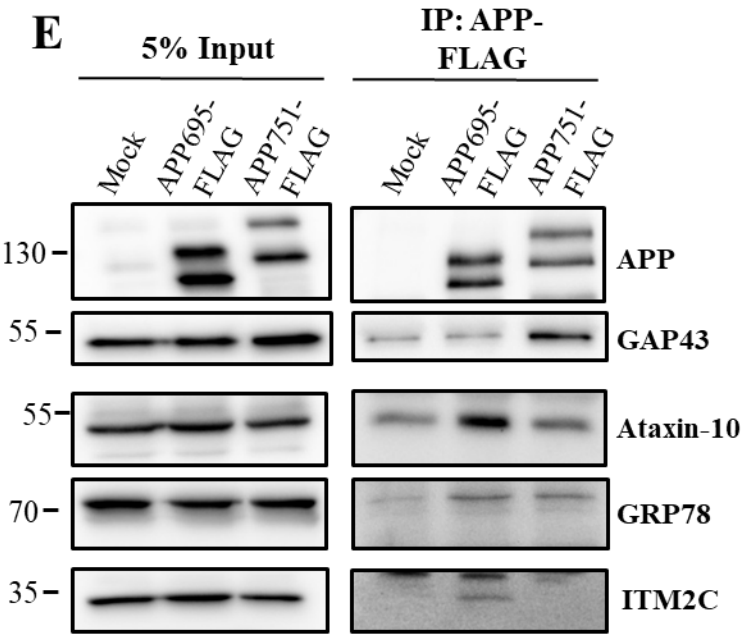
E
5% Input
IP: APP-FLAG
Mock
APP695-FLAG
APP751-FLAG
130
APP
55
GAP43
55
Ataxin-10
70
GRP78
35
ITM2C

Figure 4

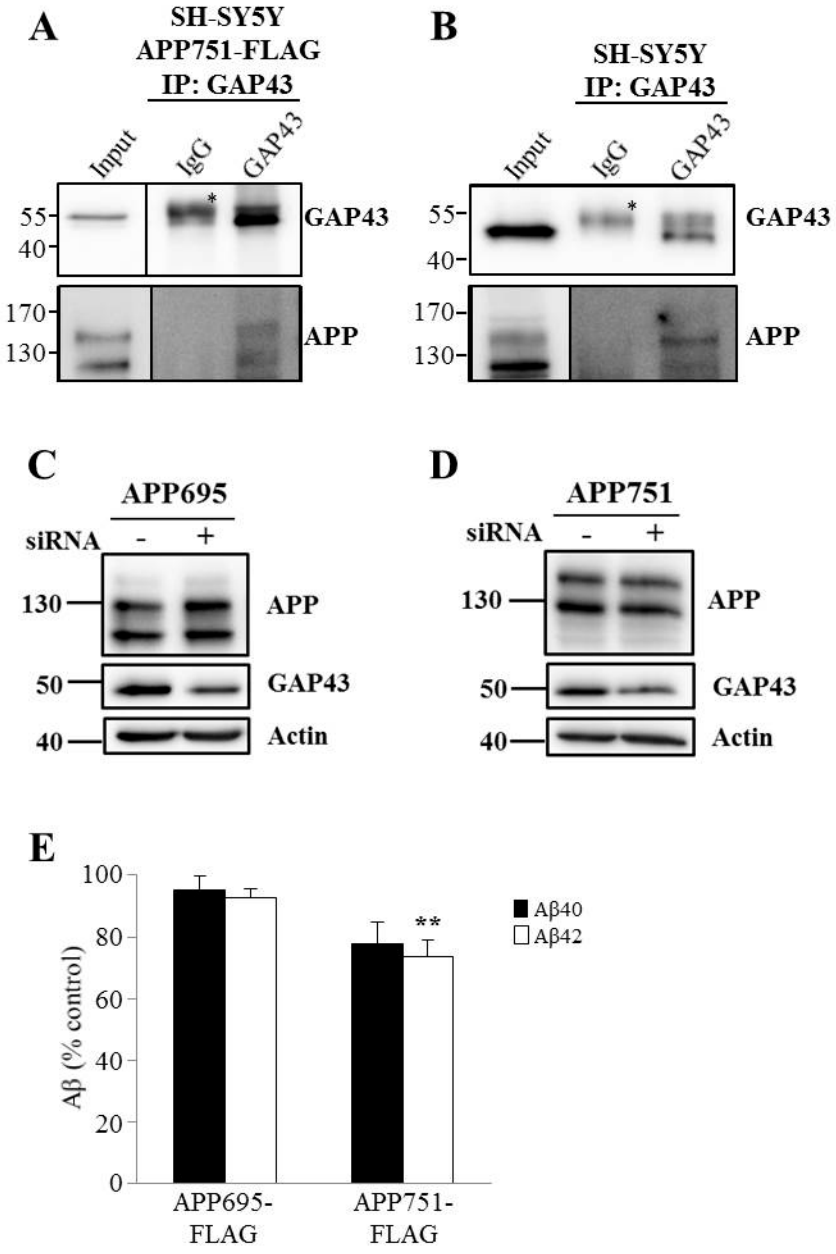
A
SH-SY5Y
APP751-FLAG
IP: GAP43
Input
IgG
GAP43
55
40
GAP43
170
130
APP
B
SH-SY5Y
IP: GAP43
Input
IgG
GAP43
55
40
GAP43
170
130
APP
C
APP695
siRNA - +
130
APP
50
GAP43
40
Actin
D
APP751
siRNA - +
130
APP
50
GAP43
40
Actin
E
100
80
60
40
20
0
Aβ (% control)
Aβ40
Aβ42
**
APP695-FLAG
APP751-FLAG

A

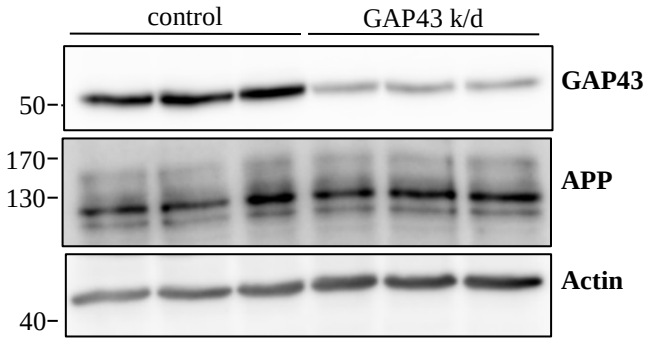
control
GAP43 k/d
50
GAP43
170
130
APP
Actin
40

B

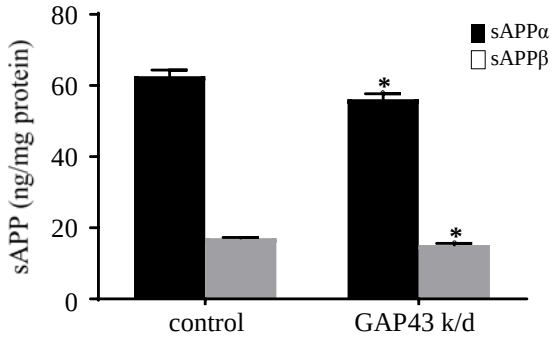
sAPP (ng/mg protein)
80
60
40
20
0
sAPPα
sAPPβ
*
*
control
GAP43 k/d

C

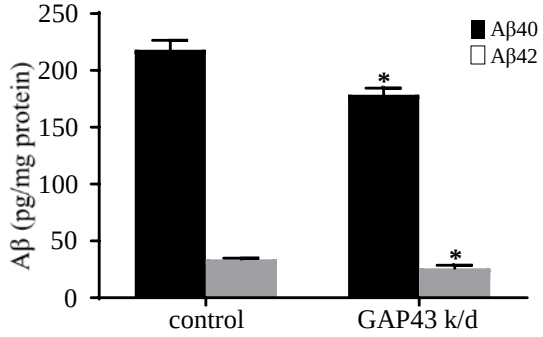
Aβ (pg/mg protein)
250
200
150
100
50
0
Aβ40
Aβ42
*
*
control
GAP43 k/d